J Biomol NMR (2008) 40:213–217
DOI 10.1007/s10858-008-9218-6

NMR STRUCTURE NOTE

NMR structure note: alkaline proteinase inhibitor APRin from *Pseudomonas aeruginosa*

Sengodagounder Arumugam · Robert D. Gray · Andrew N. Lane

Received: 7 December 2007 / Accepted: 24 December 2007 / Published online: 24 January 2008
© Springer Science+Business Media B.V. 2008

Biological context

The alkaline proteinase inhibitor (APRin) from *Pseudomonas aeruginosa* is an 11.5-kDa, high affinity, high specificity inhibitor of the serralysin class of zinc-dependent proteinases secreted by several Gram-negative bacteria (Feltzer et al. 2000). The inhibitor APRin is co-secreted from the bacterium presumably to prevent adventitious proteolysis of host proteins during the secretion process. The serralysins are mechanistically and structurally related to the matrix metalloproteinases (Morihara et al. 2000), and the active site zinc atom is accessible through a tunnel to the enzyme surface. These enzymes are capable of degrading a variety of host proteins and thereby enhance the pathogenicity of these organisms (Morihara and Homma 1985).

The X-ray structure of the proteinase-APRin complex revealed that the five N-terminal inhibitor residues occupy the extended substrate binding site of the enzyme and that the terminal amino group (Ser) coordinates to the catalytic zinc of the enzyme (Hege et al. 2001). These residues are essential for inhibitor activity (Feltzer et al. 2000). However, there is no known structure of the free inhibitor, and the conformational properties of the N-terminal region of the protein are unclear (Feltzer et al. 2003). Metalloproteinase inhibitors are of considerable biological interest as they are involved in regulating Zn metalloproteinase activity in numerous contexts including tissue destruction in pseudomonal infections, tumor metastases, and autoimmune diseases such as rheumatoid arthritis. Knowledge of the mechanism of action of these inhibitors could lead to new approaches to the preparation of therapeutically useful compounds for the treatment of these and other metalloproteinase-dependent diseases.

Electronic supplementary material The online version of this article (doi:10.1007/s10858-008-9218-6) contains supplementary material, which is available to authorized users.

S. Arumugam · A. N. Lane (✉)
J.G. Graham Brown Cancer Center, University of Louisville, Louisville, KY 40202, USA
e-mail: anlane01@louisville.edu

R. D. Gray
Department of Biochemistry and Molecular Biology, University of Louisville, Louisville, KY 40202, USA

Methods and results

Materials

APRin was expressed as a fusion protein with the pelB signal peptide of *E. coli* using the IPTG-inducible plasmid pET22b+ (Novagen, Madison, WI) and purified from the periplasm of *E.coli* BL21(DE3) cells as previously described (Feltzer et al. 2000). For ^{15}N-labeled and ^{15}N/^{13}C-labeled protein, the method of Marley et al. (2001) was used. The growth medium was replaced by M9 minimal medium supplemented with $(^{15}NH_4)_2SO_4$ (1 g l^{-1}) and ^{12}C or $^{13}C_6$ D-glucose (4 g l^{-1}) as the sole nitrogen and carbon sources. Protein residues 6–10 were replaced with glycines as previously described (Feltzer et al. 2000).

Methods

NMR spectroscopy

For NMR, protein samples were prepared in 20 mM Na phosphate, 0.1 M KCl, pH 6.5. All NMR spectra were recorded in 5 mm Shigemi tubes at 25°C on 14.1 T or 18.8

T Varian Inova spectrometers. For the $^{15}N/^{12}C$ protein the concentration was 0.8 mM, and for the $^{15}N/^{13}C$ protein, the concentration was 1.7 mM. NMR Spectra of the ^{15}N-labeled Glycine variant were recorded at 0.9 mM. All NMR spectra were acquired in phase sensitive mode with solvent suppression by Watergate (Piotto et al. 1992). Spectra were processed using NMRPIPE (Delaglio et al. 1995). Prior to Fourier transformation the data were zero filled to increase resolution and a shifted sine-squared function was applied in all dimensions. Forward linear prediction was used to extend the time domain data in the ^{15}N and ^{13}C dimensions. Spectra were analyzed using Sparky (T. D. Goddard and D. G. Kneller, SPARKY 3, University of California, San Francisco).

Structural restraints were derived from isotope-edited 2D and 3D ^{13}C and ^{15}N-edited NOESY-HSQC spectra using mixing times of 100 and 150 ms. Backbone torsion angles were determined from the heteronuclear chemical shifts determined from triple resonance 3D experiments as described (Arumugam et al. 2005) using the program TALOS (Cornilescu et al. 1999) and from the intensities in the HNHB spectrum. These were used primarily to check the validity of the values estimated using TALOS (Cornilescu et al. 1999).

Residual dipolar couplings were obtained using partially oriented samples with alkylPEG/hexanol (Ruckert and Otting 2000) and measuring the splittings in coupled HSQC spectra compared with the isotropic values.

APRin contains a single disulfide between C26 and C49. Standard bond distances for C–S and S–S bond distances were used to constrain the disulfide linkage.

Dynamical information was obtained by ^{15}N relaxation measurements on the ^{15}N-labeled sample. Spin-lattice (R_1) and spin-spin (R_2) relaxation rate constant were measured with suppression of dipole–dipole CSA cross-correlation effects (Kay et al. 1992). For the R_1 measurements, 6 delays of 0.01, 0.15, 0.3, 0.5, 0.75 and 1 s were used and 0.01, 0.02, 0.05, 0.09, 0.13 and 0.17 s for the R_2 experiments, with relaxation delays of 3 and 2.7 s, respectively. The peak intensities were fitted to an exponential decay function. The heteronuclear NOE was measured by recording two interleaved spectra, one with saturation of the protons and the other without saturation. The relaxation delay for the ^{15}N experiment was 3 s. Relaxation data were analyzed as described previously (McIntosh et al. 2000). The CSA contribution was calculated using an average value of 170 ± 17 ppm (Hall and Fushman 2006).

Structure calculations

Three-dimensional structures were calculated following established protocols using rMD with XPLOR-NIH incorporating residual dipolar couplings (Schwieters et al. 2006). Briefly this comprised high temperature (2500 K) simulated annealing from an extended chain using 100 initial random number seeds, with a minimal force field. The temperature was gradually lowered (25 K per step) to 100 K and the relative strength of the restraints increased. The folded structures were then ordered according to potential energy and restraint violation energy. Residual dipolar couplings were introduced for improvement of the structures, and also as a check on the overall conformation. These rdc-checked structures were then finally refined by restrained energy minimization, and the top 20 were used for conformational analysis including distributions of torsion angles and Ramachandran analysis using PROCHECK (Laskowski et al. 1996). The structures have been deposited to BMRB accession number 11015, PDB ID code 2rn4.

Structure

1700 distances were obtained using the isotope-separated NOESY spectra. In addition, 47 torsion angle restraints were derived from the combination of the database searching approach TALOS (Cornilescu et al. 1999) and intensity measurements. 83 residual dipolar couplings for NH vectors were obtained as described in the Methods. An additional 36 H-bond interactions were identified from slowly exchanging amide protons in D_2O solution, NOEs and initial structure calculations, making a total of 1866 restraints (Table 1). As expected, the highest restraint density is in the core of the molecule, with a very low density for residues 1–8 and the two C-terminal residues.

A family of solution structures that satisfied all of the experimental restraints was obtained using Xplor-NIH, including the residual dipolar couplings. The structures were ordered according to overall and potential energy, and the top 20 were accepted for further analysis. An overlay of the best 10 structures is shown in Fig. 1. The core of the molecule, (residues 8–105), shows a well-ordered conformation, with an rmsd to the mean structure of 0.88 ± 0.16 Å for the backbone atoms. The stereochemistry is well defined, with no significant violations of restraints or poor energy terms. Overall there is good agreement between the solution and X-ray structures for the ϕ, ψ and $\chi 1$ angles of residues 8–100. The rmsd between the mean NMR structure and the X-ray structures for residues 8–105 is 0.92 Å (backbone) and 1.5 Å (all heavy atoms). Significant differences in the core are restricted to the loops Q19–A24, W53–S56, E72–L76, Q84–G87 and Q92–G96, as shown in Fig. 2.

Table 1 Statistics of the refinement

Number of restraints	1702
NOEs	3064
Intraresidue	20
Sequential interresidue (i−j) = 1	484
Medium range (i−j ≤ 4)	190
Long range	838
Residual dipolar couplings HN	83
Dihedral restraints (TALOS)	50
H-bonds	36
Disulfide bond	1
RMSD from mean	1.25 ± 0.31 Å (all residues) backbone atoms
	1.62 ± 0.23 Å (all residues) heavy atoms)
RMSD residue 8–105	0.62 ± 0.10 Å (backbone)
	1.08 ± 0.10 Å (heavy atoms)
RMSD to X-ray structure (8–105)	1.05 Å (Backbone)
	1.58 Å (heavy atoms)

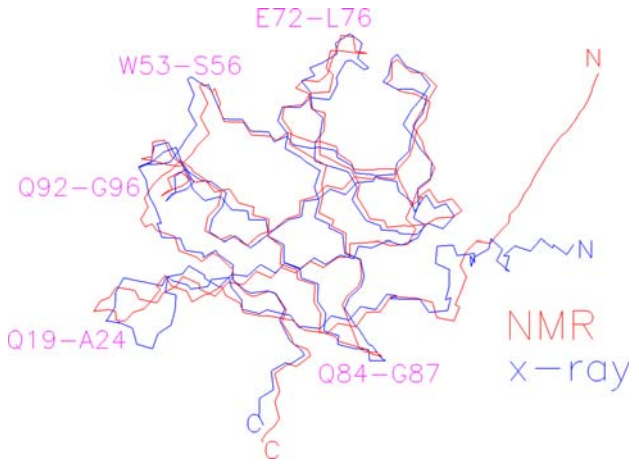

Fig. 2 Overlay of the mean NMR structure on the X-ray structure of APRin in the complex with the alkaline protease (Hege et al. 2001)

Dynamics

We have measured the ^{15}N relaxation rates under the same conditions. The core of the molecule (8–105) shows on average a heteronuclear NOE of 0.85, with a tendency to increased scatter and lower values toward the C-terminal half of the molecule. The ratio R_2/R_1 for most residues was between 4 and 5, with a small number of outliers that represent an exchange term (large R_2, normal R_1) e.g. residues 18, 50 and 95, or enhanced dynamics, cf. residues 6 and 25. The mean R_2 value is 10 ± 2 s^{-1}, and the NOE is near the maximum of 0.8 expected for a compact globular protein. Taken with the R_1 and NOE values, and excluding the outliers, we estimate an effective rotational correlation time of 5 ± 0.5 ns, and low rotational anisotropy, consistent with the overall structure of the protein in solution. The rotational correlation time for hydrated sphere of molecular weight 11,400 is expected to be ca 5 ns at 298 K in water.

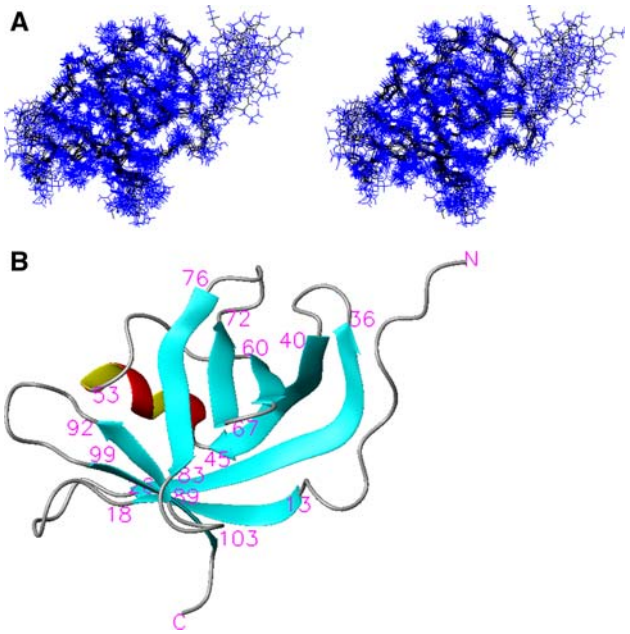

Fig. 1 Solution structures of APRin (**a**) Stereo overly of the 10 best structures determined as described in the text. (**b**) ribbon structure

N-terminal arm

The N-terminal arm, residues 1–8 did not display sharp resonances or NOEs expected of a highly dynamically disordered terminal region of a protein. Further, the backbone chemical shifts of these residues only approach random coil values at the extreme N-terminus. However, 12 NOES from the methyl group of Ala^8 were assigned, including 6 long range NOEs to core residues P^{63}, Y^{41} and W^{61}.

Both the affinity of the inhibitor for its target proteinase as well of the thermodynamic stability of the folded inhibitor are remarkably sensitive to the presence of the single-turn helix A (residues 8–11). For example, substitution of the wild-type -Ser^6-Ala-Ser-Asp-Leu^{10}-with five glycine residues results in a decrease of 1000-fold in affinity for the enzyme partner (Feltzer et al. 2000), a decrease in T_m of 8°C, and an increase in the ΔG^o of unfolding of 6 kcal/mol (Gray et al. 2005). Figure 3 shows HSQC spectra of the wild type and the variant Gly-substituted protein. In the wild-type protein, the resonances for the N-terminal residues are weak or absent. However,

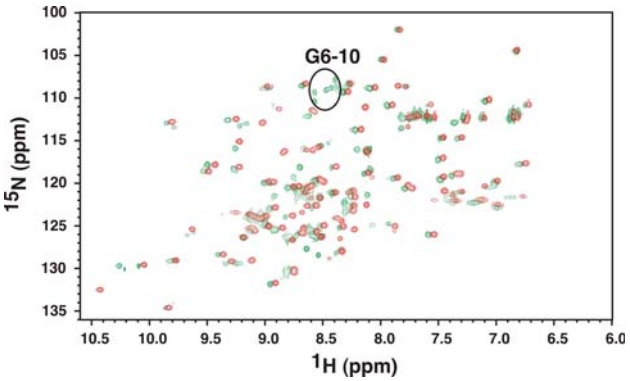

Fig. 3 HSQC of the Gly variant The ^{15}N-^{1}H HSQC spectra of wt and the glycine variant were recorded as described in the Methods. The resonances of the G6–10 substitution are circled

in the Gly substituted protein, sharp resonances for Gly appear in the HSQC spectrum in the expected positions, consistent with random coil values. This argues against the wild type having rapid NH exchange with the solvent, but rather a conformational exchange process on the μs-ms time scale or that the peptide in this region adopts a large number of conformations that do not exchange rapidly on the chemical shift time scale.

There are additional changes in chemical shifts for residues remote from the N-terminus, including H27, L30, D32, S33, L34, G40, G45, A62, G67, A69, M79, L81, G 82, G87 and G94. This suggests that in the glycine variant N-terminal arm is dynamically disordered, whereas in the wild type, there is some interaction of the arm with this part of the protein core. Presumably this would have to be displaced for the arm to penetrate into the active site of the protease.

Discussion and conclusions

The core of the inhibitor, i.e. not including the N-terminal 8 residues ("trunk") is similar to that observed in the complex with the alkaline protease. The binding surface with the enzyme includes the N-terminal trunk, which penetrates the active site to allow the N-terminal amino group to coordinate to the catalytic zinc atom. The net affinity of the intact protein for the enzyme is extremely high, $K_d = 4$ pM (Feltzer et al. 2003) and although truncation of the N-terminus cause a substantial loss in affinity(Feltzer et al. 2000), there remain numerous interactions with the β-sheet surface. What is not clear from the crystallography is the nature of the N-terminal trunk prior to binding. Is it (i) an extended chain, pre-organized to penetrate the protease active site, (ii) a completely dynamically disordered random coil, (iii) some other structure folded back on the core of the inhibitor, or, (iv) some combination of these. The NMR data clearly rule out both of the extreme cases (i) and (ii), as these would give rise to highly characteristic NMR signatures (Wishart et al. 1995; Cornilescu et al. 1999). In the former case, the ordered extended chain (which would not be expected to be stable) would give rise to non-random ^{13}C backbone chemical shifts and very characteristic NOE patterns (Cavanagh et al. 1996) that were not observed. In contrast, a random coil dynamically disordered on the sub-nanosecond timescale, would also give rise to characteristic ^{13}C chemical shifts, very sharp resonances and characteristic NOE patterns (Dyson and Wright 2005), which again were not observed. Indeed, although the chemical shifts are close to random coil values, the intensity of the peaks in HSQC and triple resonance spectra was very low compared with similar residues in the core suggesting the possibility of a disordered, quasi extended chain, that does not adopt a unique conformation. This is consistent with a lack of observable long range NOEs from these residues. The Glycine variant increased the dynamic nature of the trunk adjacent to the first helix in the APRin, indicating that in the uncomplexed state the N-terminal arm may interact with the enzyme binding surface. This would imply that the enzyme effectively displaces the strand that enters the catalytic binding site and allows optimal contact between the two proteins. It is interesting in this regard that the truncated mutants and also the glycine variants have a substantially lower melting temperature than the wild type inhibitor, indicating stabilisation of the global fold by this protein region. This is further supported in part by detailed MD simulations based on the X-ray structures (Feltzer et al. 2003; R. D. Gray unpublished data).

Acknowledgements This work was supported by the Kentucky Challenge for Excellence (to ANL). NMR spectra were recorded at the JG Brown Cancer Center NMR Facility with support from The National Science Foundation EPSCoR grant # EPS−0447479 and the Brown Foundation.

References

Arumugam S, Gray RD, Lane AN (2005) H-1, N-15 and C-13 assignments of the alkaline proteinase inhibitor APRin from *Pseudomonas aeruginosa*. J Biomol NMR 31:265–266

Cavanagh J, Fairbrother WJ, Palmer AG, Skelton AGNJ (1996) Protein NMR spectroscopy principles and practice. Academic Press, San Diego

Cornilescu G, Delaglio F, Bax A (1999) Protein backbone angle restraints from searching a database for chemical shift and sequence homology. J Biomol NMR 13:289–302

Delaglio F, Grzesiek S, Vuister GW, Zhu G, Pfeifer J, Bax A (1995) Nmrpipe—a multidimensional spectral processing system based on unix pipes. J Biomol NMR 6:277–293

Dyson HJ, Wright PE (2005) Intrinsically unstructured proteins and their functions. Nature Rev Mol Cell Biol 6:197–208

Feltzer RE, Gray RD, Dean WL, Pierce WM (2000) Alkaline proteinase inhibitor of *Pseudomonas aeruginosa*—interaction of

native and N-terminally truncated inhibitor proteins with Pseudomonas metalloproteinases. J Biol Chem 275:21002–21009

Feltzer RE, Trent JO, Gray RD (2003) Alkaline proteinase inhibitor of *Pseudomonas aeruginosa*—a mutational and molecular dynamics study of the role of N-terminal residues in the inhibition of Pseudomonas alkaline proteinase. J Biol Chem 278:25952–25957

Gray RD, Trent JO (2005) Contribution of a single-turn alpha-helix to the conformational stability and activity of the alkaline proteinase inhibitor of *Pseudomonas aeruginosa*. Biochemistry 44:2469–2477

Hall JB, Fushman D (2006) Variability of the N-15 chemical shielding tensors in the B3 domain of protein G from N-15 relaxation measurements at several fields. Implications for backbone order parameters. J Am Chem Soc 128:7855–7870

Hege T, Feltzer RE, Gray RD, Baumann U (2001) Crystal structure of a complex between *Pseudomonas aeruginosa* alkaline protease and its cognate inhibitor—inhibition by a zinc-NH_2 coordinative bond. J Biol Chem 276:35087–35092

Kay LE, Nicholson LK, Delaglio F, Bax A, Torchia DA (1992) Pulse sequences for removal of the effects of cross-correlation between dipolar and chemical-shift anisotropy relaxation mechanism on the measurement of heteronuclear T_1 and T_2 values in proteins. J Magn Reson 97:359–375

Laskowski RA, Rullmann JAC, MacArthur MW, Kaptein R, Thornton JM (1996) AQUA and PROCHECK-NMR: programs for checking the quality of protein structures solved by NMR. J Biomol NMR 8:477–486

Marley J, Lu M, Bracken C (2001) A method for efficient isotopic labeling of recombinant proteins. J Biomol NMR 20:71–75

McIntosh PB, Taylor IA, Frenkiel TA, Smerdon SJ, Lane AN (2000) The influence of DNA binding on the backbone dynamics of the yeast cell-cycle protein Mbp1. J Biomol NMR 16:183–196

Morihara K, Homma J (1985) Bacterial enzymes and virulence bacterial enzymes and virulence I. Holder. CRC Press, Boca Raton, pp 41–47

Morihara K, Hata Y, Okuda K (2000) Serralysin Zn-metalloproteinases—structure, function, secretion pathway, and pathogenicity. Seikagaku 72:16–25

Piotto M, Saudek V, Sklenar V (1992) Gradient-tailored excitation for single-quantum NMR spectroscopy of aqueous solutions. J Biomol NMR 2:661–665

Ruckert M, Otting G (2000) Alignment of biological macromolecules in novel nonionic liquid crystalline media for NMR experiments. J Am Chem Soc 122:7793–7797

Schwieters CD, Kuszewski JJ, Clore GM (2006) Using Xplor-NIH for NMR molecular structure determination. Prog NMR Spectrosc 48:47–62

Wishart DS, Bigam CG, Holm A, Hodges RS, Sykes BD (1995) H-1, C-13 and N-15 random coil NMR chemical-shifts of the common amino-acids .1. Investigations of nearest-neighbor effects. J Biomol NMR 5:67–81